



Dinàmica d'aplicacions simplèctiques quasi-integrables.

6a Jornada de Sistemes Dinàmics de Catalunya

Barcelona, 11/10/2023.

Arturo Vieiro ^a

vieiro@maia.ub.es

Universitat de Barcelona

Departament de Matemàtiques i Informàtica

^aXerrada basada en els treballs conjunts amb V.Gelfreich (Univ. Warwick)



Motivation of this work

Goal of this talk?

To develop and illustrate some tools to study the dynamics of quasi-integrable **analytic** exact-symplectic maps of $\mathbb{R}^d \times \mathbb{T}^d = \mathbb{R}^d / \mathbb{Z}^d$

$$F_\varepsilon : \begin{cases} \bar{I} = I + \varepsilon a(I, \varphi), \\ \bar{\varphi} = \varphi + \omega(I) + \varepsilon b(\bar{I}, \varphi) \pmod{1}, \end{cases}$$

implicitly defined by the generating function

$$S(\bar{I}, \varphi) = \bar{I} \varphi + h_0(\bar{I}) + \varepsilon s(\bar{I}, \varphi), \quad h_0 \text{ convex function, } h'_0(I) = \omega(I),$$

through the relations $I = \partial S / \partial \varphi$, $\bar{\varphi} = \partial S / \partial \bar{I}$.

We want to study the long term (Nekhoroshev) global stability properties of F_ε and perform a careful (local/global) exploration of the geometry of the phase space and diffusive properties (numerical tools).

Nekhoroshev estimates

Consider $0 < \varepsilon < \varepsilon_0$ and denote $(I_k, \varphi_k) = F_\varepsilon^k(I_0, \varphi_0)$, $k \in \mathbb{Z}$.

For $d = 1$, the rotational invariant curves divide the 2D phase space and there is no global diffusion if ε is small enough (e.g. Chirikov standard map).

For $d \geq 2$, the complement of KAM d -dimensional discrete tori is connected and trajectories might travel along phase space (Arnold diffusion).

^a **Nekhoroshev estimate:** $|I_k - I_0| \leq R(\varepsilon)$ when $|k| \leq T(\varepsilon)$, where $R(\varepsilon) \sim \varepsilon^\beta$ and $T(\varepsilon) \sim \exp(c/\varepsilon^\alpha)$ with $\alpha = \beta = 1/(2(d + 1))$.

Our main interest is not in the result itself (which is well-known) but in the **methodology**: we shall recover this estimate from an **explicit construction of the slow variable directly from the iterates of the map (IVFs)**.

^aS.Kuksin and J.Pöschel, *On the inclusion of analytic symplectic maps in analytic Hamiltonian flows and its applications*. Seminar on Dynamical Systems 12:96–116, 1994.

P.Lochak and A.I.Neishtadt, *Estimates of stability time for nearly integrable systems with a quasiconvex Hamiltonian*, Chaos 2, 1992.

Phase space geometry ($d=2$)

Diffusion along phase space takes place basically along single resonances but multiple resonances play a key role in an explanation of the Arnold diffusion.

To illustrate this we consider the map T_δ defined by the generating function

$$S(\psi_1, \psi_2, J_1, J_2) = \psi_1 \bar{J}_1 + \psi_2 \bar{J}_2 + \delta \mathcal{H}(\psi_1, \psi_2, \bar{J}_1, \bar{J}_2), \text{ where}$$
$$\mathcal{H}(\psi_1, \psi_2, \bar{J}_1, \bar{J}_2) = \frac{J_1^2}{2} + a_2 J_1 J_2 + a_3 \frac{J_2^2}{2} + \cos(\psi_1) + \epsilon \cos(\psi_2),$$

through the relations $J_i = \partial S / \partial \psi_i$, $\bar{\psi}_i = \partial S / \partial \bar{J}_i$, $i = 1, 2$:

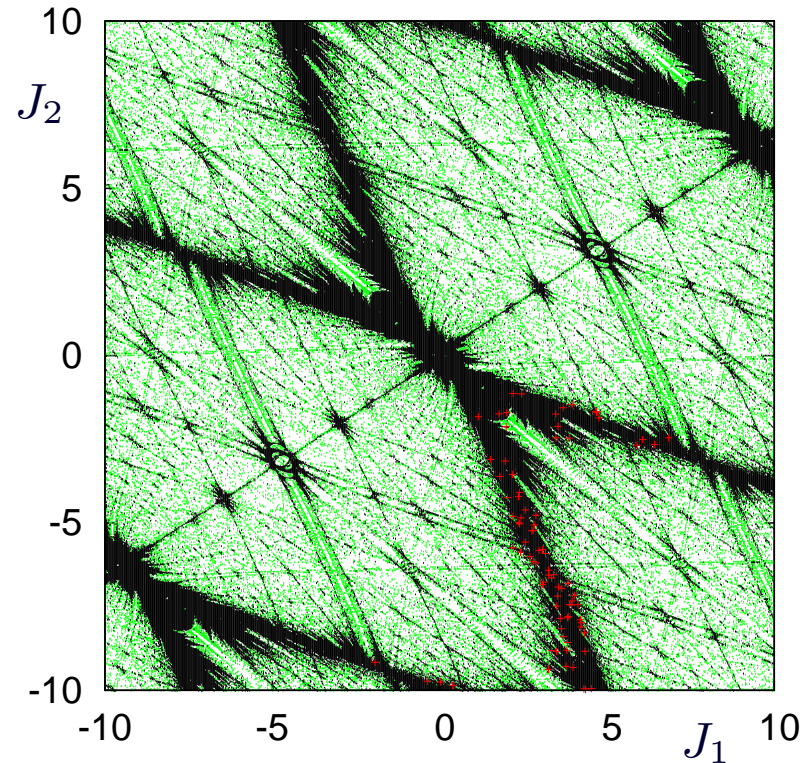
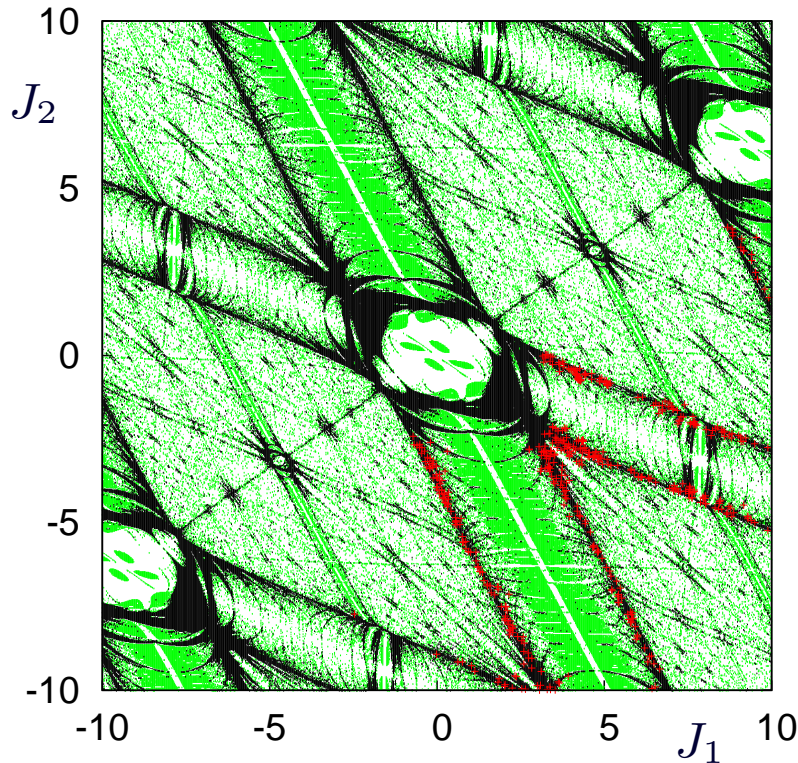
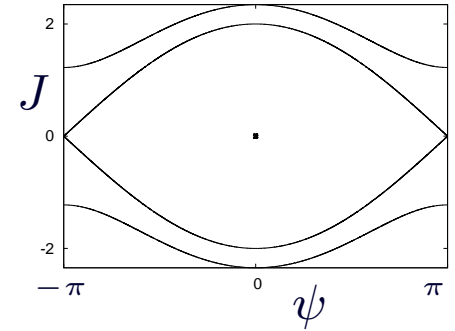
$$T_\delta : \begin{pmatrix} \psi_1 \\ \psi_2 \\ J_1 \\ J_2 \end{pmatrix} \mapsto \begin{pmatrix} \bar{\psi}_1 \\ \bar{\psi}_2 \\ \bar{J}_1 \\ \bar{J}_2 \end{pmatrix} = \begin{pmatrix} \psi_1 + \delta(\bar{J}_1 + a_2 \bar{J}_2) \\ \psi_2 + \delta(a_2 \bar{J}_1 + a_3 \bar{J}_2) \\ J_1 - \delta \sin(\psi_1) \\ J_2 - \delta \epsilon \sin(\psi_2) \end{pmatrix}$$

\mathcal{H} resembles to a “two-pendulum” Hamiltonian and T_δ is δ -close to the Id.

Single resonance: NHIC \approx ric of a pendulum system \times saddle of the other

Double resonance: \approx (ψ_1, J_1) -pendulum \times (ψ_2, J_2) -pendulum

Role of double resonances



$\delta = \epsilon = a_2 = 0.5, a_3 = 1.25$. Lyap. exp. (megno): **black** \rightarrow chaotic, **green** \rightarrow weakly chaotic, white \rightarrow regular. **Red**: Iterates of the point $(0, 0, 4.5, -5.25)$ in a slice of width 5×10^{-3} around $\psi_1 = \psi_2 = 0$ (left plot) and $\psi_1 = \psi_2 = \pi$ (right plot). Total number of iterates= 10^{12} .

Lochak approach steps

The role of maximum (*double* if $d = 2$) resonances is emphasized in the Lochak-Neishtadt approach to proof the Nekhoroshev estimates. The map F_ϵ is the isoenergetic Poincaré return map of a $(d + 1)$ -dof analytic Hamiltonian

$$\hat{H}(\hat{I}, \hat{\psi}, \epsilon) = \hat{H}_0(\hat{I}) + \epsilon \hat{H}_1(I, \hat{\phi}, \epsilon), \text{ where}$$
$$\hat{I} = (I, I_3), \hat{\psi} = (\psi, \psi_3), \hat{w}(\hat{I}) = (w(I), 1), \text{ and } \hat{H}_0(\hat{I}) = \hat{\omega}(\hat{I}) \cdot \hat{I}.$$

1. Construct a **covering of the action space** by open neighbourhoods of a finite number (depending on ϵ) of unperturbed tori bearing periodic motions (maximum resonances).
2. Normalize the Hamiltonian around a periodic orbit: by successive changes of variables (**averaging procedure**) the non-resonant terms of H can be annihilated within an **exponentially small error** \rightsquigarrow **slow observable**
3. Use **convexity** to guarantee exponential stability in the neighbourhood.

Indirect procedure: The evaluation of the local (in each domain of the covering) slow observable (to measure diffusion) requires a transformation to NF.

“Our Lochak-like approach”

Note that, for a map $F_\varepsilon = F_0 + \mathcal{O}(\varepsilon)$, $F_0(I, \varphi) = (I, \varphi + \omega(I))$, if $n\omega(I_*) \in \mathbb{Z}^d$ for some $n \in \mathbb{N}$ and $I_* \in \mathbb{R}^d$ then $I = I_*$ is a torus invariant by F_0 foliated by invariant n -periodic orbits. Note that near I_* the map F_ε^n becomes **close-to-the-identity**.

Our proof of the Nekhoroshev theorem is based on **a refinement of Neishtadt’s averaging theorem** of approximation of a close-to-Id map by an autonomous Hamiltonian flow with an **exponential small error**.

Our construction of an approximating vector field is based on the **discrete averaging and interpolating vector fields** (IVFs): it is **explicit** in terms of iterates of the map, can be easily implemented numerically and **avoids changes of variables**.

Next we study **close-to-Id maps and IVFs**. Later we will come back to the stability problem for near-integrable maps.



Close-to-identity maps and IVFs

Interpolating vector fields (IVFs)

Let $f : \mathcal{U} \mapsto \mathbb{R}^s$ real analytic on $\mathcal{U} \subset \mathbb{R}^s$ open domain. Let $m \geq 0$ and assume that there is $\mathcal{U}_0 \subset \mathcal{U}$ such that $f^k(\mathcal{U}_0) \subset \mathcal{U}$ for $0 \leq k \leq m$. Denote $x_k = f^k(x_0)$, $x_0 \in \mathcal{U}_0$. There is a unique polynomial $P_m(t; x_0)$ of order m in t such that $P_m(k; x_0) = x_k$ for $0 \leq k \leq m$.

Definition. The interpolating vector field (IVF) X_m at $x \in \mathcal{U}_0$ is the velocity vector of the interpolating curve at $t = 0$, that is, $X_m(x_0) = \partial_t P_m(0, x_0)$.

1. $X_m(x_0) = \sum_{k=0}^m p_{mk} f^k(x_0)$ is a weighted average of the iterates with p_{m0} the Harmonic number and for $k > 1$

$$p_{mk} = (-1)^{k+1} \frac{m+1-k}{k(m+1)} \binom{m+1}{k}.$$

2. **Numerics:** higher accuracy for symmetric interpolation nodes around x_0 .
(i.e. we consider p_{2m} s.t. $x_k = p_{2m}(t_k; x_0, \epsilon)$, $\forall t_k = \epsilon k$, $|k| \leq m$.)

IVF-embedding a near-Id map into a flow

Consider a smooth one-parameter near-Id family of maps

$$f_\epsilon(x) = x + \epsilon G_\epsilon(x).$$

and interpolation nodes $t_k = \epsilon k$.

1. X_m extends continuously to $\epsilon = 0$ and $X_m(x, 0) = G_0(x)$ the limit v.f.
2. f_ϵ is close to the time- ϵ flow of the IVF: ^a If $f_\epsilon \in \mathcal{C}^{2m+1}$ and $\mathcal{U}_0 \subset \mathcal{U}$ compact, then the IVF X_{2m} is uniformly bounded in \mathcal{U}_0 for $|\epsilon| < \epsilon_0$ and

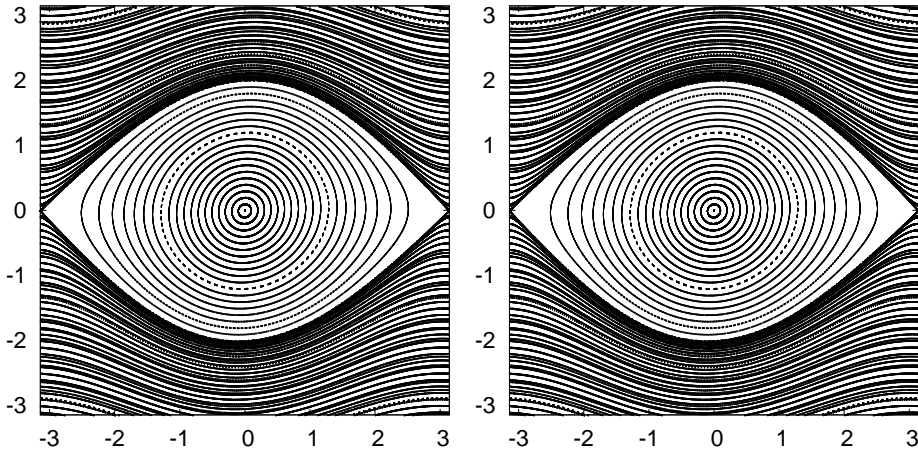
$$F_\epsilon(x) = \Phi_{X_{2m}}^\epsilon(x) + O(|\epsilon|^{2m+1}).$$

Remark. This result was obtained by relating IVF with the “suspension+averaging” procedure (not explicit!). If f_ϵ is analytic in a complex neighbourhood of \mathcal{U}_0 and we choose $m \sim \epsilon^{-1}$ then we proved that the IVF interpolates f_ϵ with an exponentially small error.

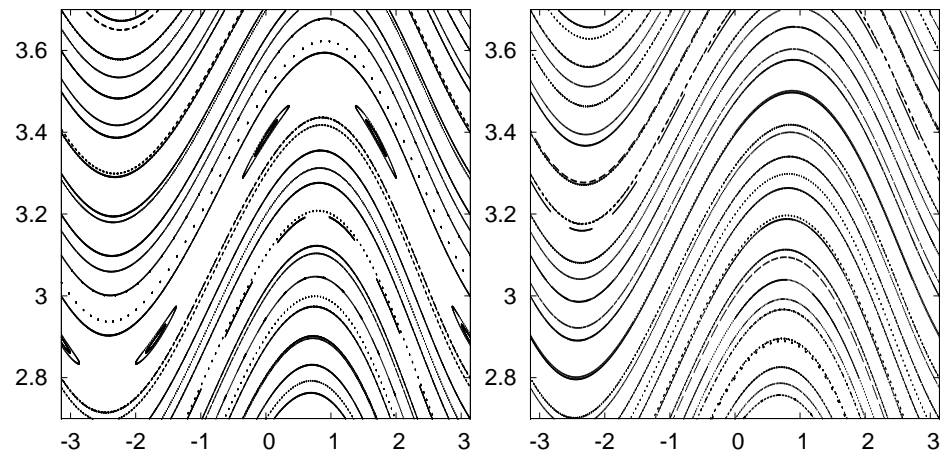
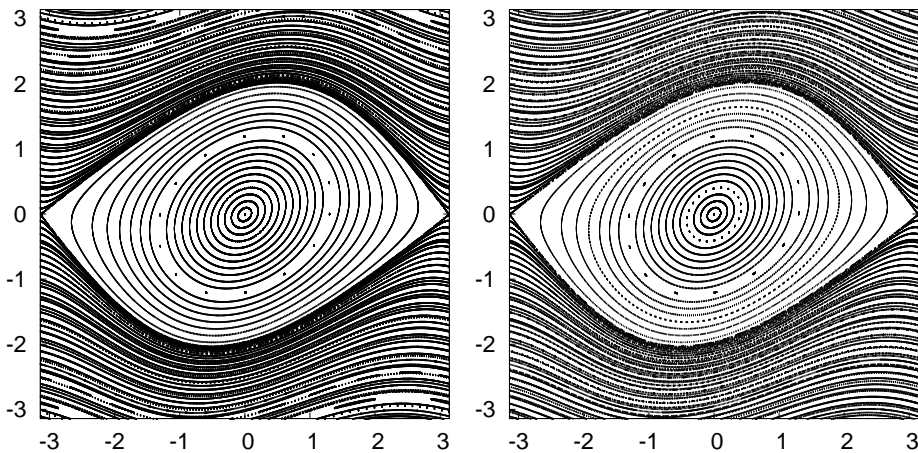
^aV.Gelfreich and AV, *Interpolating vector fields for near identity maps and averaging*, Nonlinearity 31(9), 4263–4289, 2018

Example: Chirikov standard map on $S^1 \times \mathbb{R}$

$$M_\epsilon : (x, y) \mapsto (\bar{x}, \bar{y}) = (x + \epsilon \bar{y}, y - \epsilon \sin(x)), \quad \epsilon \in \mathbb{R}.$$



$\epsilon = 0.1$, same 200 i.c. Left: 10^3 iterates of M_ϵ . Right: RK78 integration of X_{10} up to $t = 10^3$ plotting every $\Delta t = 0.1$. **No visual differences!**



Bottom: $\epsilon = 0.5$, left plots for M_ϵ and right plots for X_{10} .

IVF-exponential embedding of a near-Id map

Let f an exact symplectic map ϵ -close-to-Id in $D = D_0 + \delta$ a complex δ -neighbourhood of $D_0 \subset \mathbb{R}^{2d}$. Assume it admits a generating function $G(P, q) = Pq + S(P, q)$ such that S can be analytically continued onto D and denote by $\epsilon = \|\nabla S\|_D$. As before X_m is the IVF.

Theorem [GV23]. If $m = \left\lfloor \frac{\delta}{6e\epsilon} - d \right\rfloor \geq 1$, then

$$\|\Phi_{X_m} - f\|_{D_0} \leq 3 e^{d+2} \epsilon \exp(-\delta/(6e\epsilon)).$$

Moreover there is a Hamiltonian interpolating vector field \hat{X}_m such that

$$\|\hat{X}_m - X_m\|_{D_1} \leq 3 e^{d+1} \epsilon \exp(-\delta/(6e\epsilon)),$$

where D_1 is the $\frac{\delta}{2}$ -neighbourhood of D_0 , and

$$\|\Phi_{\hat{X}_m} - f\|_{D_0} \leq 5 e^{d+2} \epsilon \exp(-\delta/(6e\epsilon)).$$

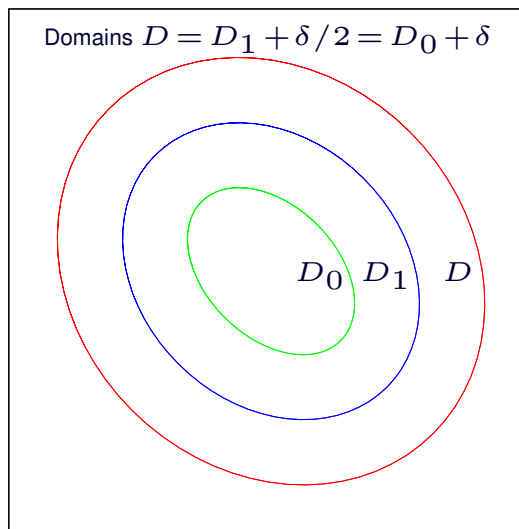
Comments on the theorem

We need to explicitly control of the constants in front of ϵ^m . Indeed, under the assumption of the theorem for every $1 \leq m < \delta/(6\epsilon) - d$ the following inequalities hold: $\|X_m\|_{D_1} \leq 2\epsilon$, $\|\hat{X}_m\|_{D_1} \leq 4\epsilon$,

$$\|\Phi_{X_m} - f\|_{D_0} \leq 3C_m^{m-1}\epsilon^m, \quad \|\Phi_{\hat{X}_m} - f\|_{D_0} \leq 5C_m^{m-1}\epsilon^m,$$

$$\|\hat{X}_m - X_m\|_{D_1} \leq 8C_m^m\epsilon^{m+1}$$

where $C_m = 6(m + d)/\delta$. The exponential bound is obtained by choosing m to minimize the error bound: $m \approx \delta/6\epsilon$.



Direct explicit proof! (sketch of ideas)

1. We embed f into a family of symplectic maps f_μ (homotopy):

$$G_\mu(P, q) = Pq + \mu S(P, q)$$

2. Choose $|\mu| < \delta / (2\epsilon(m + d))$ so that $x_j \in D$, $0 \leq j \leq m$, for all $x_0 \in D_1$. This implies analyticity of $X_{m,\mu}$.
3. The proof of the first inequality reduces to bounding the IVF $X_{m,\mu}$ of f_μ on D_1 . If $\xi = id$ and $T_f(g) = g \circ f$, one has $X_{m,\mu} = -\sum_{k=1}^m \frac{1}{k} (I - T_{f_\mu})^k \xi$, and, since $\text{val}_\mu((I - T_{f_\mu})^k \xi) \geq k$, we use the MMP to bound $X_{m,\mu}$ (decreasing the analyticity strip in μ).
4. The IVF $X_{m,\mu}$ is not Hamiltonian but the m -jet in μ

$$\hat{X}_{m,\mu} = \sum_{k=1}^m \frac{1}{k!} \partial_\mu^k X_{m,\mu} \Big|_{\mu=0} \mu^k$$

is a Hamiltonian vector field.



Obtaining Nekhoroshev estimates

Following Lochak-Neishtadt approach

We investigate iterates $(I_k, \varphi_k) = F_\varepsilon^k(I_0, \varphi_0)$ of an arbitrary initial condition. If $n\omega(I_*) \in \mathbb{Z}^d$ for some $n \in \mathbb{N}$ and $I_* \in \mathbb{R}^d$, then the equation $I = I_*$ defines a torus filled with periodic orbits of the integrable map F_0 . In a neighbourhood of $I = I_*$ we consider the lift of F_ε^n given by

$$f_\varepsilon^n : (I_0, \varphi_0) \mapsto (I_n, \varphi_n - n\omega(I_*)).$$

Trajectories of F_ε^n and f_ε^n coincide when angles are considered modulo one. Concretely, we study iterates of f_ε^n in $\mathcal{D}_0(I_*) = B(I_*, \rho_n) \times \mathbb{R}^d$, where

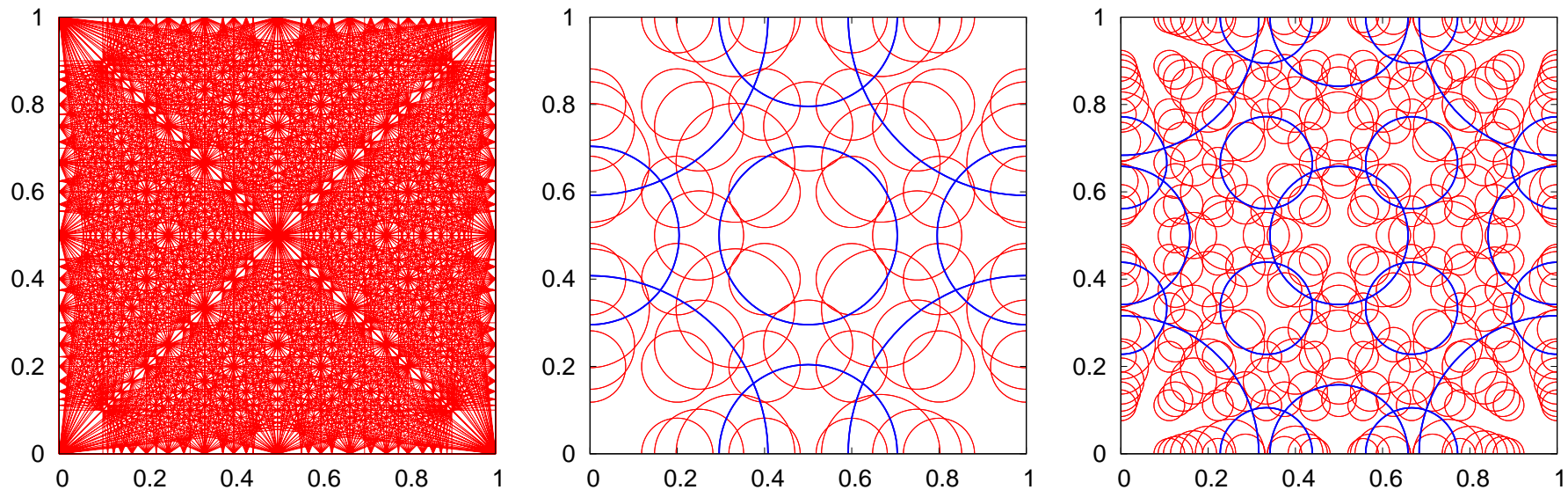
$$\rho_n = \rho_\varepsilon/n, \quad \rho_\varepsilon = \gamma N_\varepsilon^{-1/d} = \gamma \varepsilon^{1/2(d+1)}, \quad N_\varepsilon = \varepsilon^{-d/2(d+1)}.$$

The constant γ is independent of n and ε . If γ is sufficiently large these domains completely cover the domain of the map F_ε provided we consider all fully resonant tori with $n < N_\varepsilon$. This is a consequence of Dirichlet theorem on simultaneous approximation and convexity of $h'_0(I) = \omega(I)$.

Covering: frequency space

Dirichlet theorem: For any $\omega \in \mathbb{R}^d$ and any $N > 1$ there is a vector $\omega_* \in \mathbb{Q}^d$ and $n \in \mathbb{N}$ such that $1 \leq n < N$, $n\omega_* \in \mathbb{Z}^d$ and $|\omega - \omega_*| < \frac{1}{nN^{1/d}}$.

\Rightarrow the balls $B(k/n, n^{-1}N^{-1/d})$ with $k \in \mathbb{Z}^d$ and $1 \leq n < N$ cover the whole frequency space \mathbb{R}^d .



Left: Resonant lines up to order 10. Center: We consider n up to $N = 6$ and we plot a circle of radius $\frac{1}{n\sqrt{N}}$ around. Right: Same for $N = 10$. As $\epsilon \searrow 0$ larger N is needed. But to cover the resonances $(1, 0)$ and $(0, 1)$ we need periods $\ll N$.

Interpolation near a fully resonant torus

In $\mathcal{D}(I_*) = \{ (I, \varphi) \in \mathbb{C}^{2d} : |I - I_*| < 2\rho_n, |\operatorname{Im}(\varphi)| < r/2 \}$, a complex neighbourhood of $\mathcal{D}_0(I_*)$, we introduce the scaled action $I = I_* + \rho_n J$ so that the lift f_ε^n can be written as

$$\hat{f}_\varepsilon^n : \begin{cases} \bar{J} = J + \rho_n^{-1} \varepsilon \sum_{k=0}^{n-1} a(I_k, \varphi_k), \\ \bar{\varphi} = \varphi + \sum_{k=0}^{n-1} (\omega(I_k) - \omega(I_*)) + \varepsilon \sum_{k=0}^{n-1} b(I_k, \varphi_k), \end{cases}$$

which is ε_n -close-to-Id in $\mathcal{D}(I_*)$, with

$$\varepsilon_n \leq \max \{ C_1 \rho_n^{-1} n \varepsilon, C_2 n \rho_n \} \leq C_3 \varepsilon^{1/2(d+1)}.$$

By the interpolation theorem: there is $m = m(\varepsilon) \sim \varepsilon_n^{-1}$ such that the time-one map of the Hamiltonian vector field \hat{X}_m verifies

$$\left\| \hat{f}_\varepsilon^n - \Phi_{\hat{X}_m} \right\|_{B(0,1) \times \mathbb{R}^d} \leq 5e^{d+2} \exp \left(-\gamma_0 \varepsilon^{-1/2(d+1)} \right).$$

Long term stability of actions (key points)

The Hamiltonian H_m corresponding to \hat{X}_m is used to bound the actions.

1. Since \hat{f}_ε^n is exact symplectic it derives from a generating function S_n .

One has $S_n(\bar{J}, \varphi) = S_n^L(\bar{J}, \varphi) + w_n(\bar{J}, \varphi)$, where

$$S_n^L(\bar{J}, \varphi) = n\rho_n^{-1} (h_0(I_* + \rho_n \bar{J}) - h_0(I_*) - \rho_n \langle h'_0(I_*), \bar{J} \rangle)$$

If γ is large enough then $\|w_n\| \leq \nu\rho_\varepsilon/9$ where $\nu =$ convexity constant of h_0 . Relating H_m with S_n^L one can use convexity of h_0 , and adapt Lochak-Neishtadt reasoning for flows to this setting.

2. The energy change by iterate of \hat{f}_ε^n is exponentially small

$$\begin{aligned} \left\| H_m \circ \hat{f}_\varepsilon^n - H_m \right\| &= \left\| H_m \circ \hat{f}_\varepsilon^n - H_m \circ \Phi_{\hat{X}_m} \right\| \leq \|H'_m\| \left\| \hat{f}_\varepsilon^n - \Phi_{\hat{X}_m} \right\| \\ &= \|\hat{X}_m\| \left\| \hat{f}_\varepsilon^n - \Phi_{\hat{X}_m} \right\| \leq 20\varepsilon_n e^{d+2} \exp\left(-\gamma_0 \varepsilon^{-1/2(d+1)}\right). \end{aligned}$$

\rightsquigarrow If $|I_0 - I_*| \leq \sqrt{\nu}\rho_n/6\|w'\|$, then $|I_{kn} - I_*| \leq \rho_n$ for $0 \leq kn \leq T_{\text{Nek}}$, where $T_{\text{Nek}} \geq \frac{n\nu}{240\varepsilon_n e^{d+2}} \exp\left(\gamma_0 \varepsilon^{-1/2(d+1)}\right) \implies$ Nekhoroshev estimates.

Exploring diffusion

Diffusion - general picture

Consider F_ε near-integrable 4D map, then:

1. **Near a double resonance:** Closer to a tori bearing periodic orbits of short period n , the distance-to-Id of the lift f_ε^n of the near-integrable map F_ε^n becomes smaller. Hence, h_m^N is well-preserved for a much larger number of iterates. This prevents orbits from getting close to or escaping from a small neighbourhood of the double resonance in a moderate number of iterates.
2. **Single resonances:** For double resonances of different enough order, hence with large n , h_m^n is badly preserved since f_ε^n is far-from-Id. This is responsible of the fast drift along single resonances typically observed.

Computation of an adiabatic invariant

Numerically we do not compute the Hamiltonian from \hat{X}_m . Instead we directly compute an adiabatic invariant h_m s.t. $J\nabla h_m \approx X_m = (X_m^i)_{i=1,\dots,2d}$ as follows. Consider a near-Id map f_ϵ such that $f_\epsilon^*(\omega) = \omega$ where $\omega = \sum_{i=1}^d dx_i \wedge dx_{i+d}$ standard symplectic form. Let $\nu_m = \omega(X_m, \cdot) = \sum_{1 \leq i \leq d} (X_m^i dx_{i+d} - X_m^{i+d} dx_i)$. Given $p_0 \in D_0$ define for every $x \in D_0$

$$h_m^\epsilon(x; p_0) = \int_{\gamma(p_0, x)} \nu_m, \quad \text{along a path } \gamma(p_0, x) \text{ from } p_0 \text{ to } x.$$

Lemma[GV23]. If f_ϵ is defined on $\mathbb{T}^2 \times \mathbb{R}^2$ and h_m is computed along a piecewise path with straight segments parallel to the (ordered) axes, then there is a constant c_1 and a periodic function c_2 s.t.

$$\tilde{h}_m^\epsilon(x; p_0) = h_m^\epsilon(x; p_0) - c_1(x^0 - p_0^0) - c_2(x^0)(x_1 - p_0^1),$$

is globally well-defined on $\mathbb{T}^2 \times \mathbb{R}^2$.

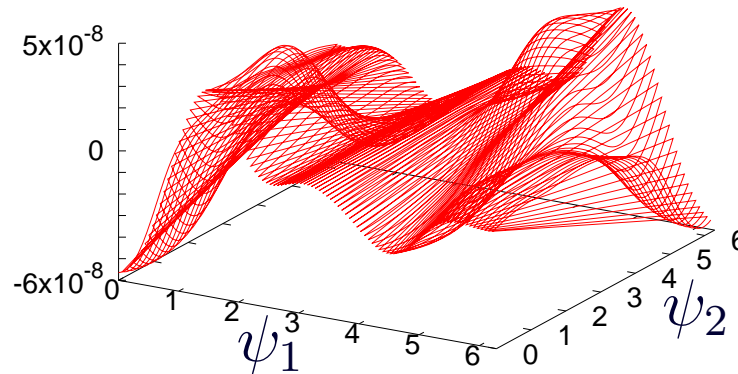
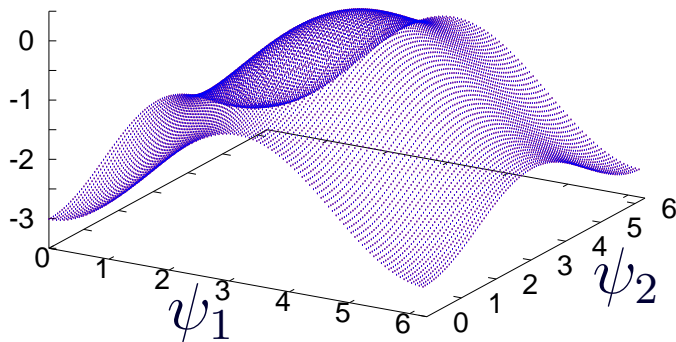
Correction of h_m to be periodic

Lemma [GV18]. For any compact $\tilde{D}_0 \subset D_0$ and $\forall x \in \tilde{D}_0$, one has

$$h_m(f_\epsilon(x), \epsilon) - h_m(x, \epsilon) = O(\epsilon^m),$$

i.e. h_m is **approximately preserved** for ϵ^{-m} iterates.

Remark: \tilde{h}_m is an exponentially small in ϵ correction of h_m :



We consider T_δ for $\delta = 0.2$.

Left: h_{20} and \tilde{h}_{20} of points $(\psi_1, \psi_2, 0, 0)$ with base point $p_0 = (\pi, \pi, 0, 0)$. Right: Their difference.

Remark: The behaviour is independent of the choice of p_0 .

IVFs- “Poincaré” sections to visualize dynamics

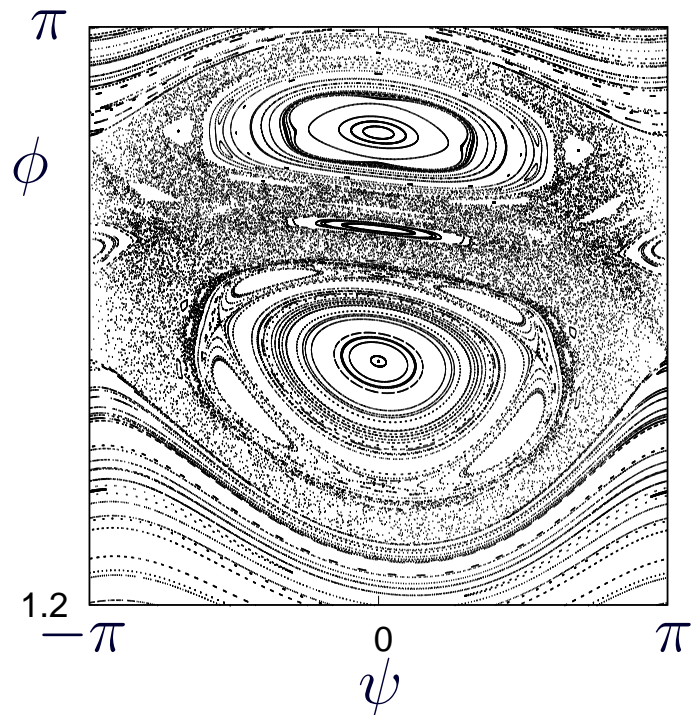
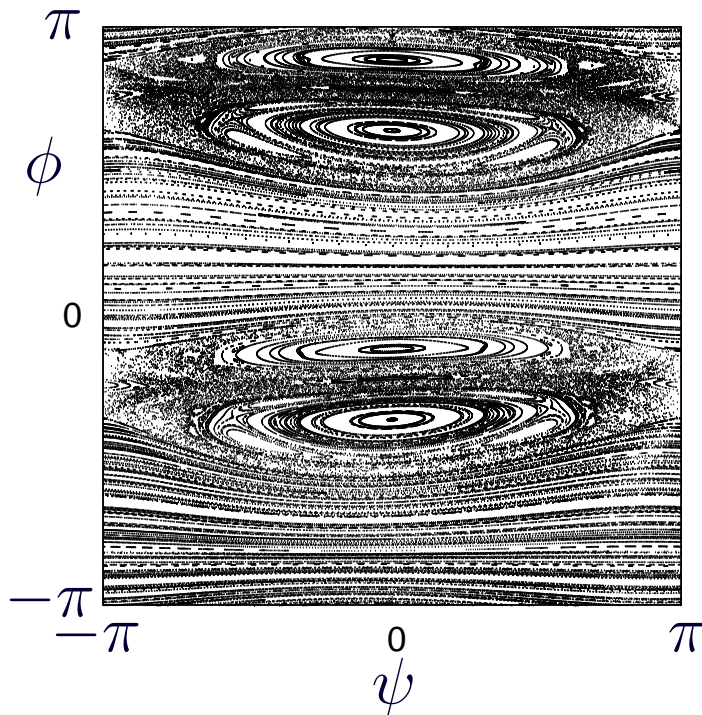
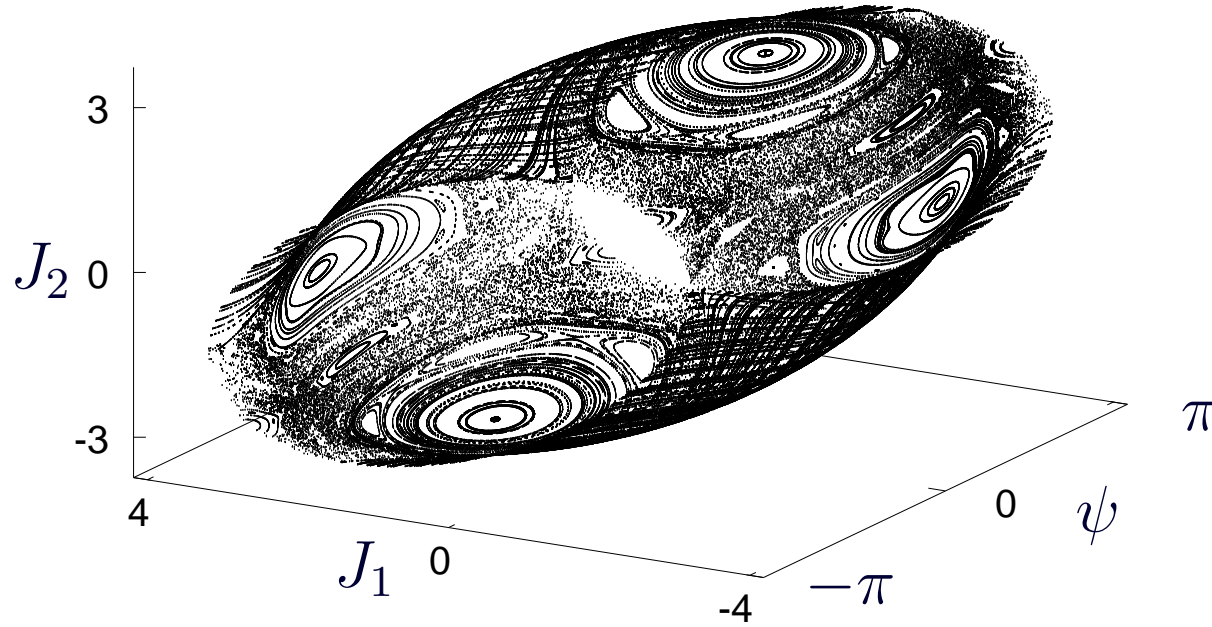
Let $g : \mathbb{R}^m \rightarrow \mathbb{R}$ smooth s.t. $\Sigma = \{x \in \mathbb{R}^m : g(x) = 0\}$ is a smooth hyper-surface of codimension one. Take $x_0 \in D_0$ and iterate $x_{k+1} = f_\epsilon(x_k)$. Assume that $g(x_k)g(x_{k+1}) \leq 0$ (crossing). If the limit vector field G_0 is (locally) transversal to Σ then, for ϵ small enough, there is a unique $t_k \in [0, \epsilon]$ such that $g(\Phi_{X_n}^{t_k}(x_k)) = 0$.

→ Plot $y_k = \Phi_{X_n}^{t_k}(x_k)$ instead of (any other projection of) x_k .

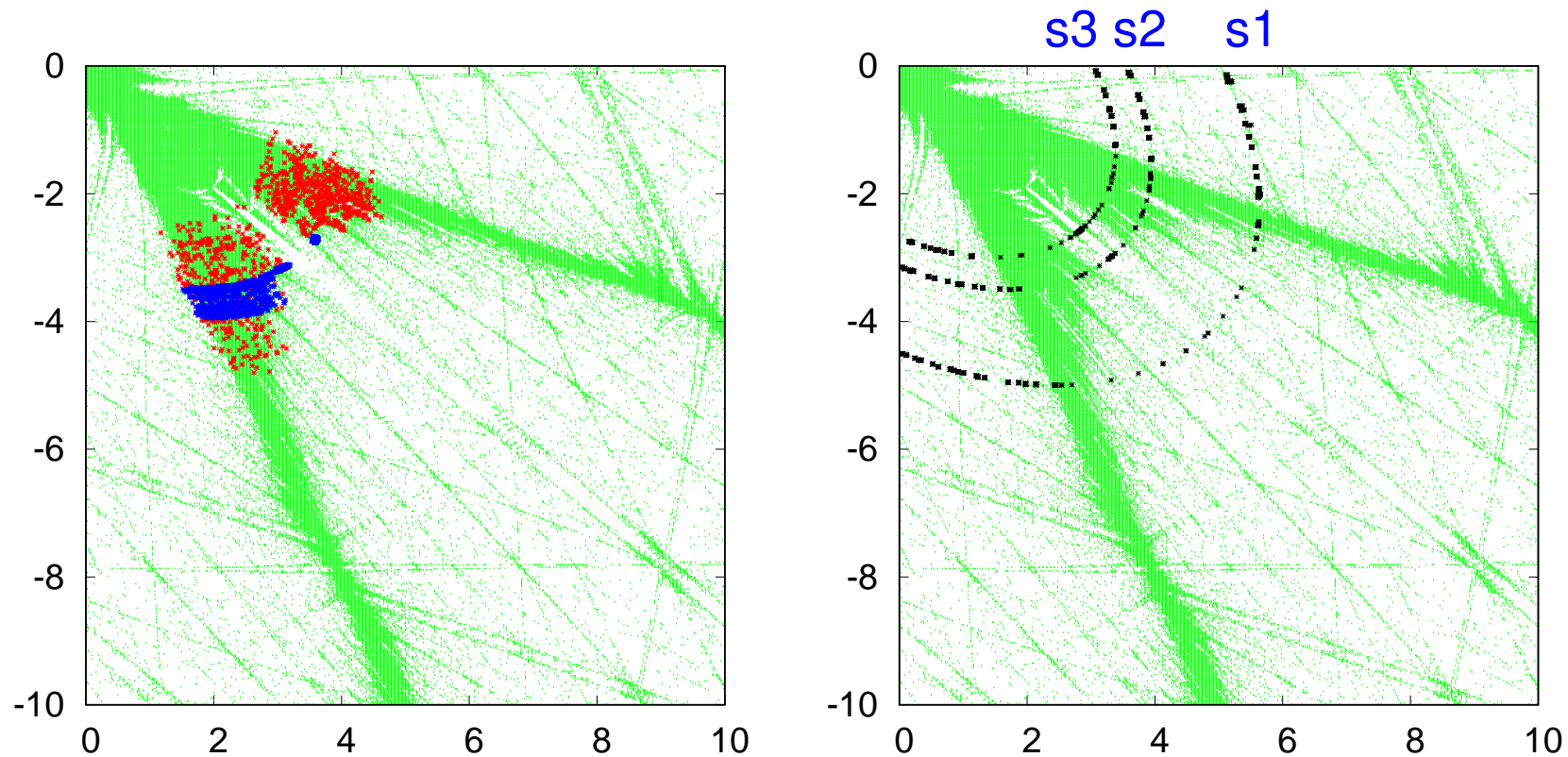
Visualizing 4D near-Id dynamics: For a map like T_δ , obtained as a discretization of $H = J_1^2/2 + a_2 J_1 J_2 + a_3 J_2^2/2 + V(\psi)$, $\Sigma = \{\psi_1 = \psi_2\}$ is a transversal section (if $|\delta|$ small enough). On a moderate time scale the iterates of $x_0 \in \mathbb{T}^2 \times \mathbb{R}^2$ remain close to the “energy” surface $M_E^m = \{x : h_m(x, p_0) = E\}$, where $E = h_m(x_0, p_0)$. At each crossing, we project onto Σ along the IVF X_n to get $y_{k_j} \in \Sigma$.

For E large enough, one has $M_E^n \cong \mathbb{T}^3$. Then $\psi = \psi_1 = \psi_2$, $\phi = \arg(J_1 + iJ_2)$ are convenient coordinates on $\Sigma \cap M_E^n \cong \mathbb{T}^2$.

T_δ , $\delta = 0.35$, 400 i.c. on $\Sigma \cap \{h_{10} = 4\}$, 500 it

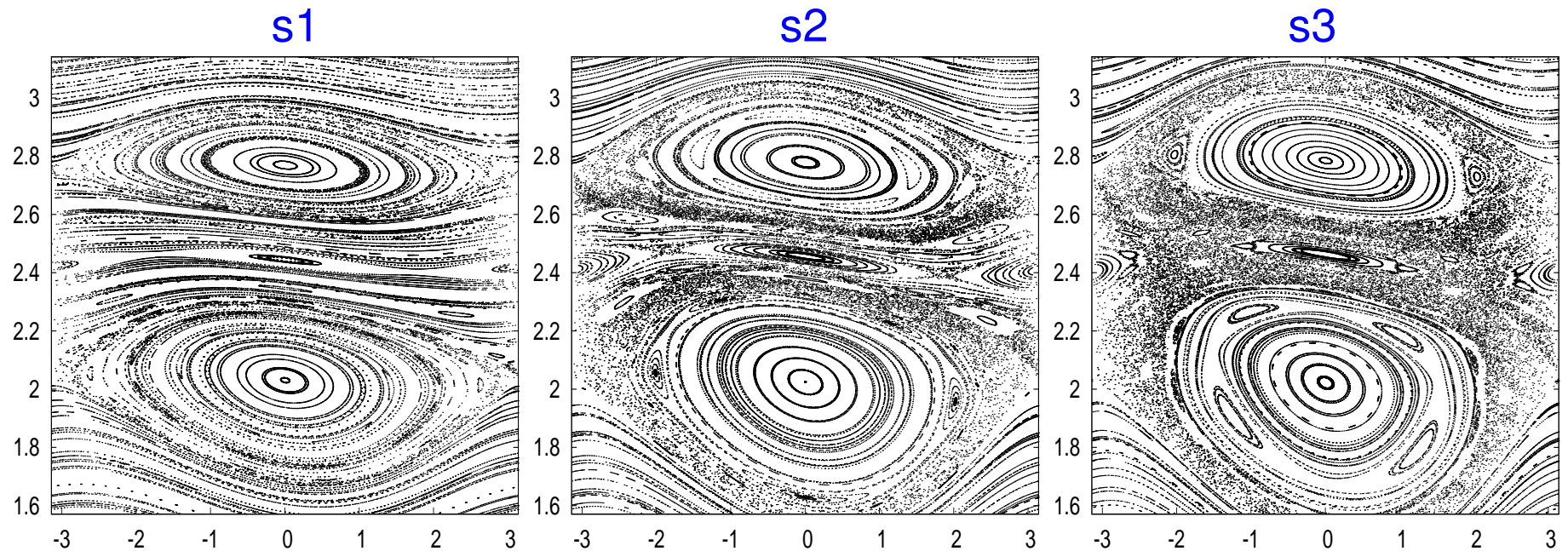


Turning at a resonant crossing



T_δ , $\delta = 0.4$. Left: IC $(3, 3, 2.136447, -3.904401)$ near $J_1 + a_2 J_2 \approx 0$. We perform around 10^8 (resp. 10^{10}) iterates and show in blue (resp. red) iterates on $\Sigma = \{\psi_1 = \psi_2\}$ with $|\psi_1 - \pi| < 0.35$. Similar for most orbits. Right: Energy levels (s1 and s2 above the level of the crossing observed).

“Poincaré” sections & last “RIC”

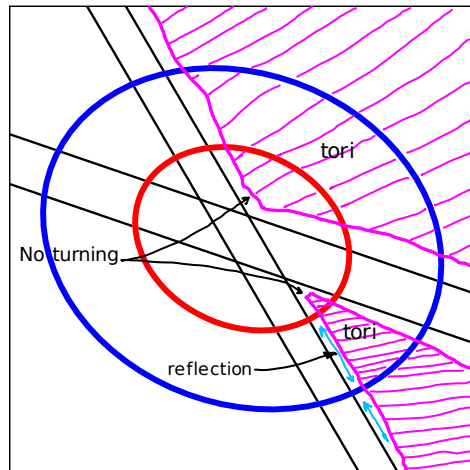


J_1	\tilde{h}_{11}^1	tori?
2.5	12.327	Y s1
2.0	7.889	Y
1.75	6.041	Y s2
1.625	5.209	N
1.5	4.439	N s3

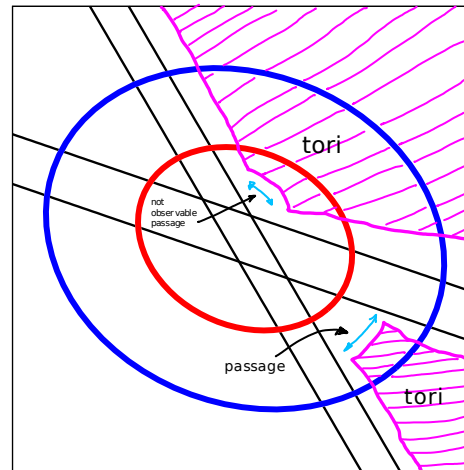
Approaching the HH-point (with $h = 0$) of the double resonance the projection “Poincaré” maps become more chaotic. The last “rotational invariant curve” is at $h \approx h(\pi, \pi, J_1, -a_2 J_1) \approx 5.209$. It corresponds to $J_1 \approx 1.625$. Numerical simulations detect passages for $1.37 \lesssim J_1 \lesssim 1.5$.

Diffusion around double resonances

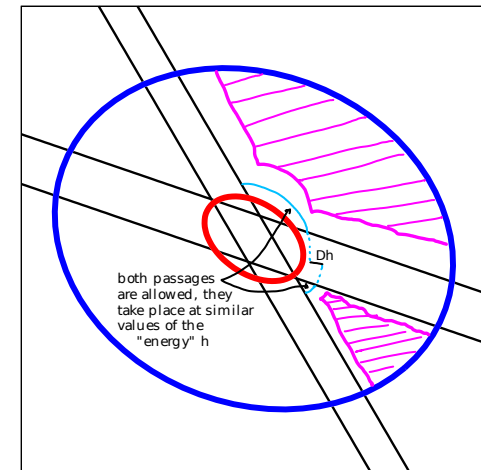
Different patterns depending on the different time-scales (i.e. depending on ϵ , the order of the resonance n and the structure of f_ϵ^n):



Reflection



Turning shorter angle



Turning around
(single resonance)

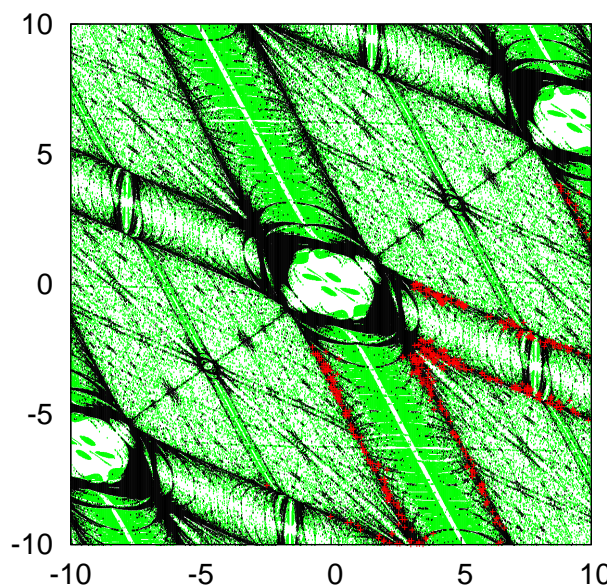
Inside red circle:

$$h_m^n \sim \text{ctant}$$

longer time-scale

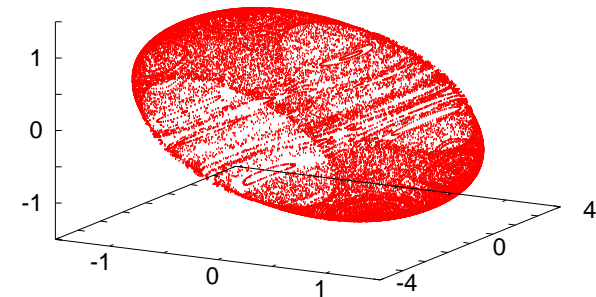
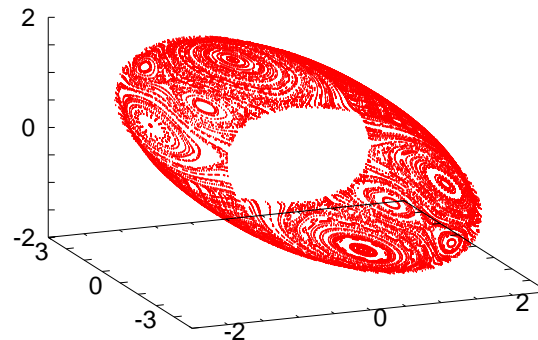
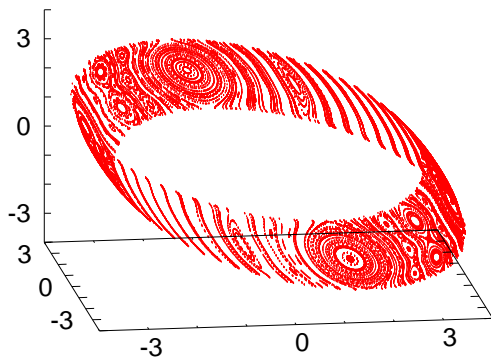
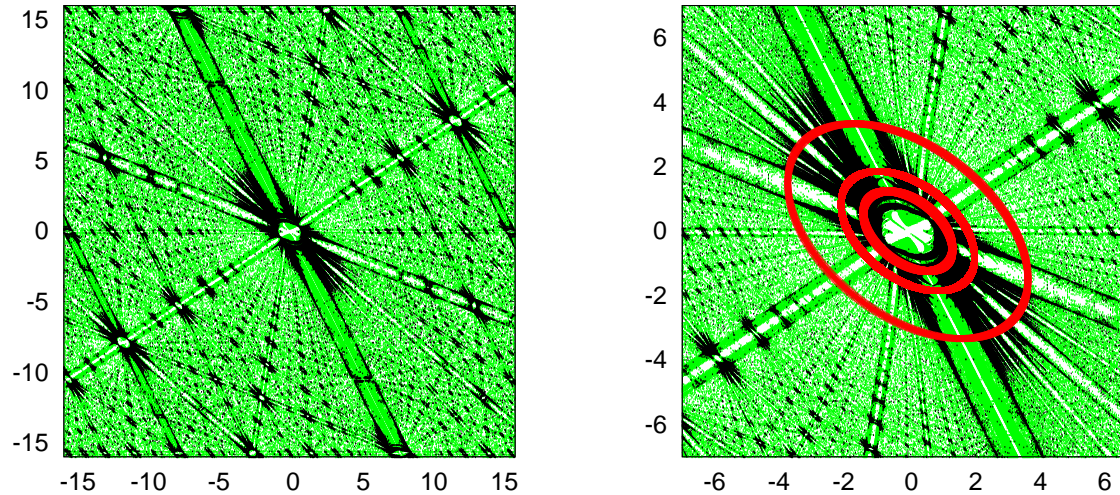
Inside blue circle:

h_m^n evolves on a
medium time-scale



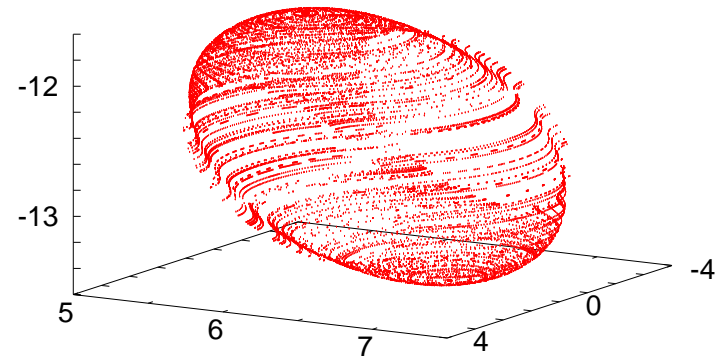
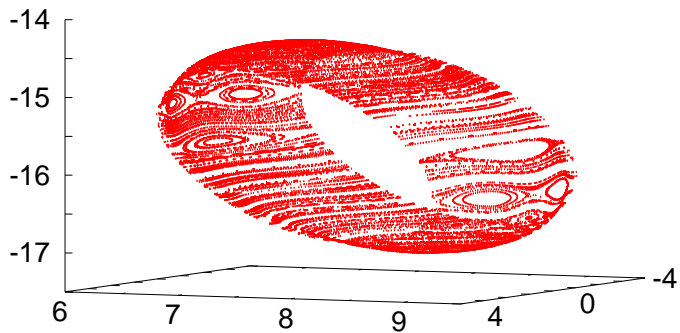
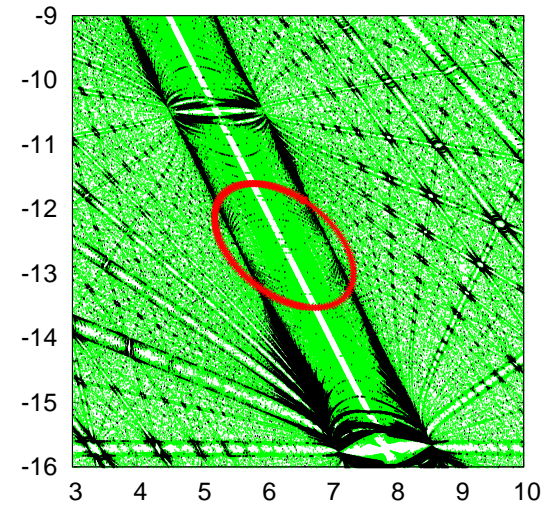
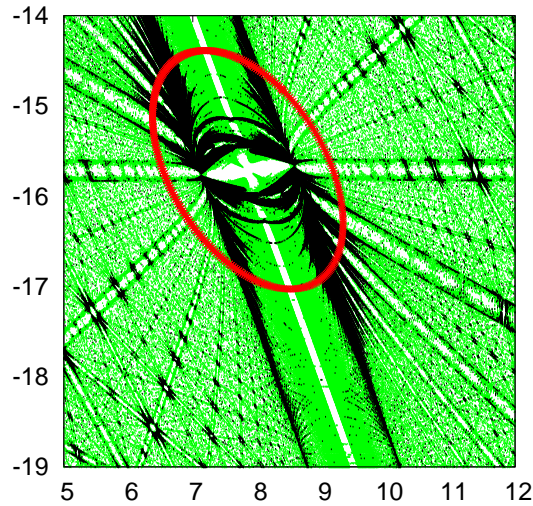
Different crossings

We use a 4D map with a potential $V(\psi) = \frac{\cos(\psi_1) + \epsilon \cos(\psi_2)}{3(\cos(\psi_1) + \epsilon \cos(\psi_2) + 3)}$, hence with **all harmonics**, and look at different resonances. Illustrations for $\delta = 0.2$.



From left to right, “Poincaré” sections using $h^{n=1}$ and $J = 1.6, 0.8, 0.4$.

Different crossings

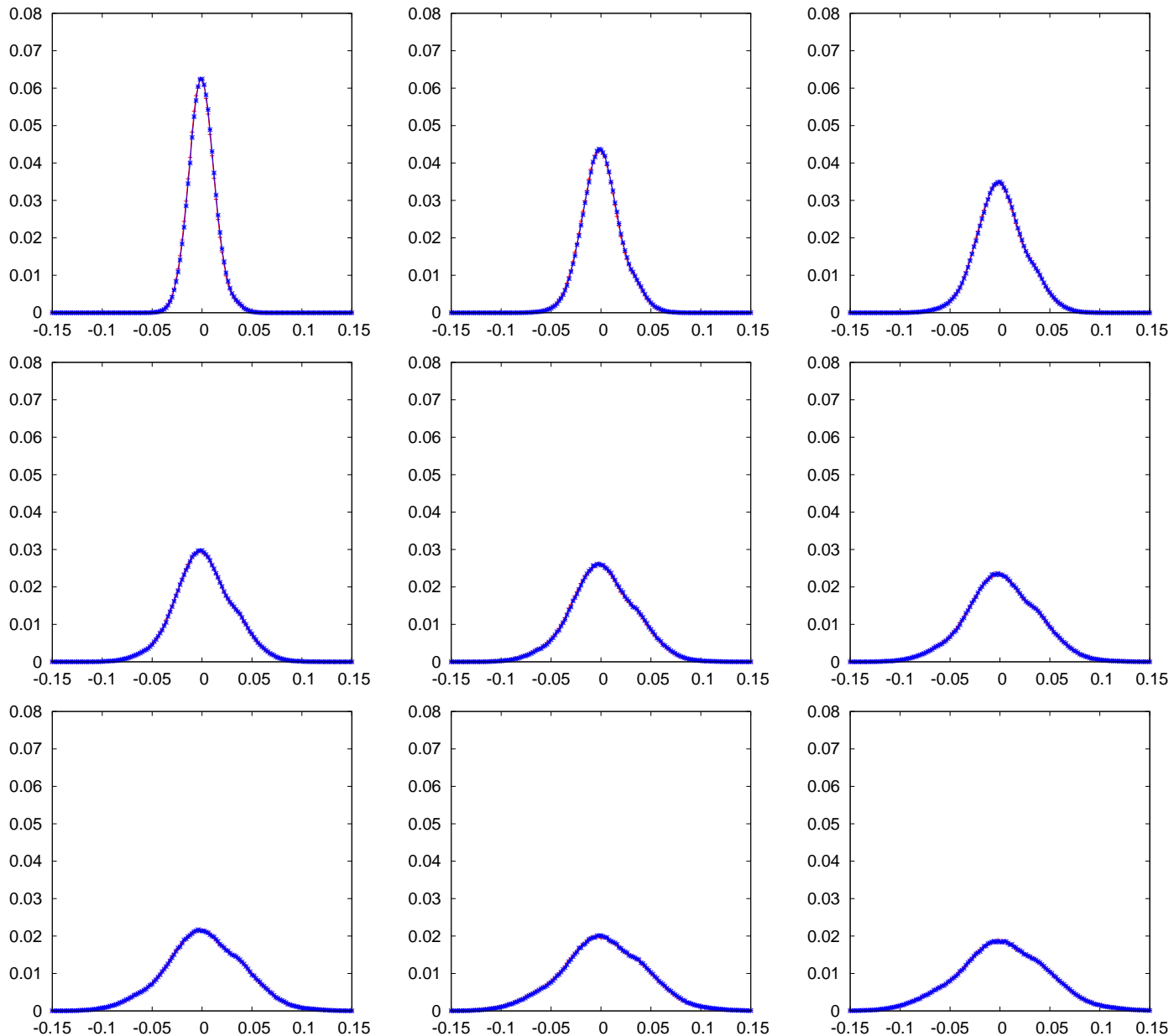


From left to right, “Poincaré” sections using $h^{n=2}$ (res 1:2, $J = 8.4$) and $h^{n=5}$ (res 2:5, $J = 6.6$)

Movie

IVFs - quantitative information on diffusion

Local diffusive properties: oscillations of h_m along a single resonance.



$T_\delta, \delta = 0.4,$
 10^6 i.c. with
 $h_{10} = 3.5,$
 $\text{nit} = k \cdot 10^6,$
 $k = 1, \dots, 9$



Locally
Gaussian
(but effect of
many crossing
resonances)



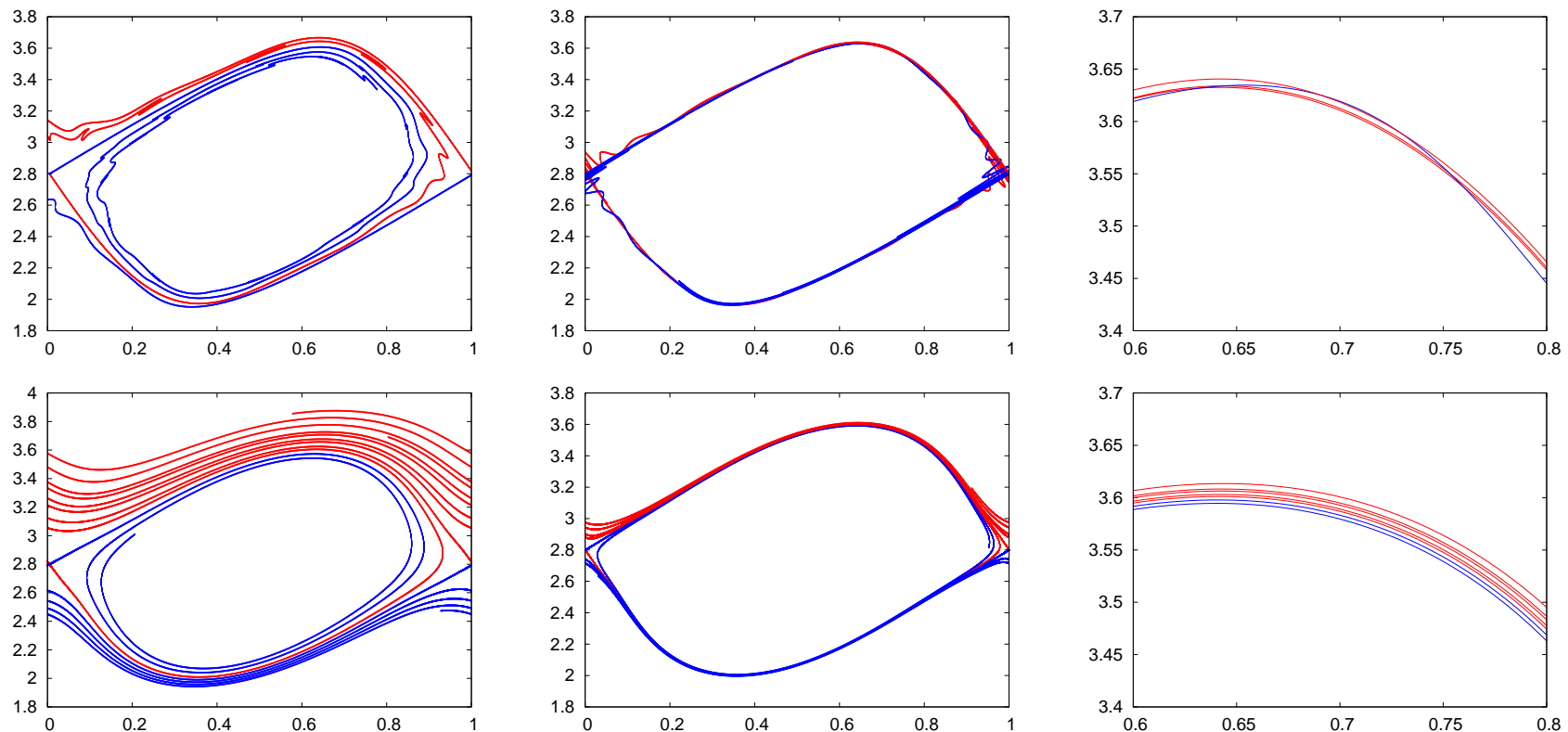
Final comments and conclusions

IVF - other settings: near-conservative dynamics

Example: Dissipative standard map ^a

$$M_{\epsilon, \delta} : (x, y) \mapsto (\bar{x}, \bar{y}) = (x + \delta \bar{y}, (1 - \epsilon)y - \delta \sin(2\pi x) + c), \quad \epsilon \in \mathbb{R}.$$

We consider $\delta \approx 3.57 \times 10^{-1}$, $\omega \approx 6.18 \times 10^{-1}$ and $\epsilon = 10^{-2}$ (left), 10^{-3} (center/right).

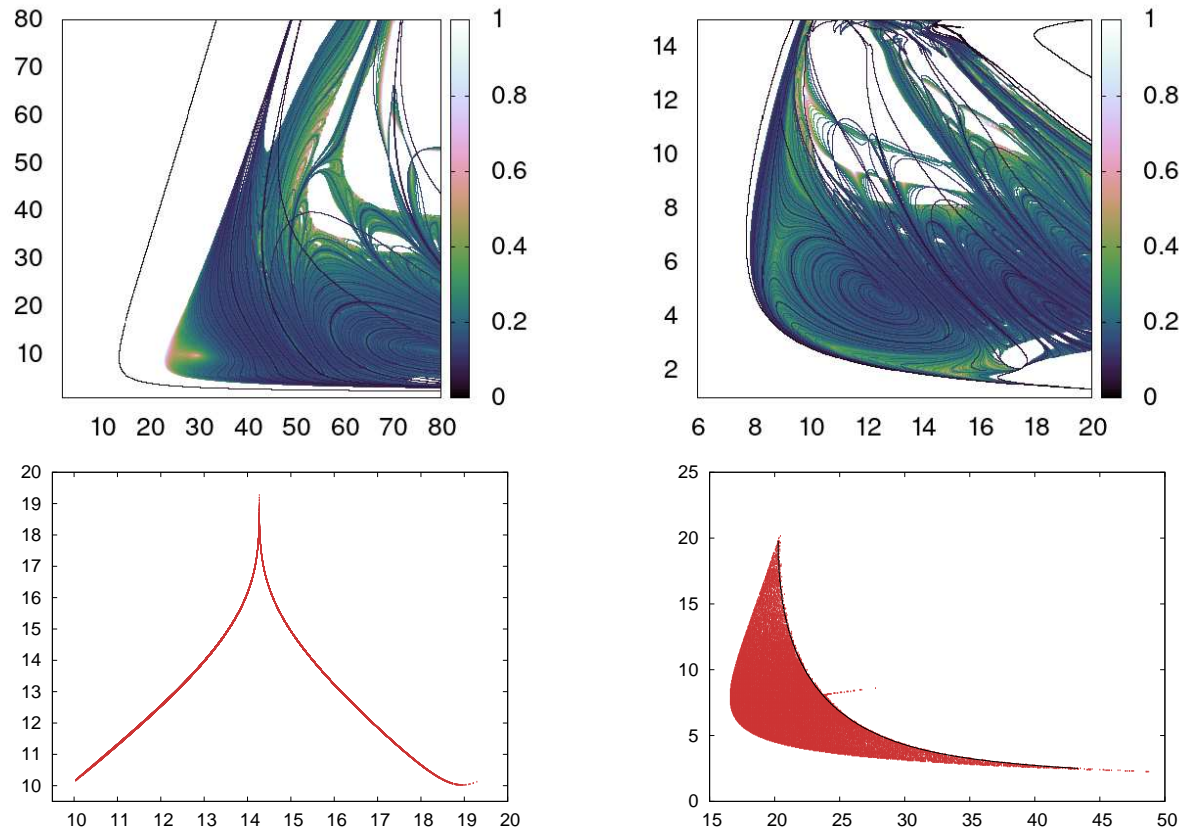


The origin is an attracting focus. Preliminary numerical exploration indicate that the probability of capture by the focus can be defined as the **ratio between the entrance/exit strips** (one can avoid homoclinics).

^aOngoing work with R.Calleja

IVF - other settings: discrete Lorenz attractors

Lorenz map: $\bar{x} = x + \delta(\sigma(y - x))$, $\bar{y} = y + \delta(\bar{x}(\rho - z) - y)$, $\bar{z} = z + \delta(\bar{x}y - 8z/3)$. ^a



For δ small, we use IVF to compute kneading diagram, (ρ, σ) -parameter space (top right $\delta = 0.001$, top left $\delta = 0.06$), reduce dynamics to 1D-“Poincaré maps” (bottom left, $\delta = 0.001$), and compute the region with pseudohyperbolic discrete Lorenz-like attractors (bottom right, $\delta = 0.01$).

^aA.Kazakov, A.Murillo, AV, K.Zaichikov, “Numerical study of discrete Lorenz-like attractors.” Submitted to RCD.

Conclusions & future work

- **IVFs – a numerical tool to study near-Id dynamics:**

We have used IVFs to investigate the key **role of double resonances** in the diffusion process. They allow to compute the **slowest variable** h_m at any point of the phase (useful for visualizations/quantitative simulations of diffusion) from simulations in **original system variables**.

- **IVFs – analytical tool to study near-Id dynamics:**

The relation of IVFs with discrete averaging allow to obtain **optimal and explicit** theoretical results: exponential embedding of a symplectic near-Id map into a Hamiltonian flow and Nekhoroshev estimates for near-integrable maps.

- **What's next? Many Arnold diffusion questions...**

- ▶ Determine ε -ranges for which the different regimes near a double resonance are observed. “last invariant torus”?
- ▶ The stochastic limit needs to be clarified, and convergence to a local Gaussian process justified. Role of high order resonances?
- ▶ Can we construct the “effective graph” of diffusion for a given IC (and for a given simulation time)? This require to adapt covering to the IC.

Thanks for your attention!!